Solid-State ^{29}Si MAS NMR Study of Titanosilicates

Mari Lou Balmer,* Bruce C. Bunker, Li Qiong Wang, C. H. F. Peden, and Yali Su

Pacific Northwest National Laboratory, Richland, Washington 99352

Received: April 28, 1997; In Final Form: August 22, 1997[⊗]

The relationship among the ^{29}Si NMR chemical shift, the number of titanium polyhedra coordinating each silicon tetrahedron, and the oxygen formal charge is examined for titanosilicates with known crystal structures. A systematic downfield chemical shift is observed when increasing numbers of titanium polyhedra coordinate a given silicon tetrahedron, which is similar to the trend seen for aluminosilicates. The chemical shift increases linearly with increasing oxygen formal charge for both titanosilicates and aluminosilicates. Summation of the oxygen formal charge accounts for effects on the chemical shift from coordination geometry, nonbridging oxygen, and cation valence. Silicates with a high oxygen formal charge, or more than one nonbridging oxygen per silicon, deviate from the linear trend observed for aluminosilicates and titanosilicates. The chemical shift/structure correlations derived from titanosilicates with known crystal structures are used to determine the local bonding configurations for a new titanosilicate, $CsTiSi_2O_{6.5}$, and for an Engelhard formulation designated ETS-4.

1. Introduction

Recent work has shown that some titanosilicate zeolites can be used to promote oxidation and hydroxylation reactions in various catalytic processes, while other unique titanosilicate structures are effective in selectively removing cesium from waste streams with high sodium concentrations.[1−3] The discovery of this promising new group of materials has stimulated efforts to synthesize new titanosilicates with acid−base and steric properties tailored to specific processes. Optimization of the properties of known titanosilicates and development of new titanosilicate structures is facilitated by a clear understanding of the crystal structures, coordination geometries, and local bonding configurations of titanium and silicon in the covalently bonded network.[4−10] Structural features such as the ring opening size or layer spacing influence steric selectivity, while the coordination geometries and local bonding configurations control the distribution of active sites, which in turn influences the acid−base properties and selectivity of the material.[11]

Information on the local bonding configuration around silicon can be obtained by solid-state nuclear magnetic resonance (NMR) spectroscopy. ^{29}Si NMR spectroscopy has been used extensively to determine the degree of anion condensation in silicates and the number of AlO_4^- tetrahedra linked to SiO_4^- tetrahedra.[12,13] Previous work has shown that there are distinct chemical shift ranges associated with the number of nonbridging oxygens or with the number of AlO_4^- tetrahedra coordinating any given silicon tetrahedron.[12−14] These relationships have been used reliably to provide both qualitative and semiquantitative information about the structures of new aluminosilicate zeolites.[14] Although a large amount of valuable ^{29}Si NMR data have been collected for aluminosilicates, relatively little information is available for titanosilicates. This scarcity of data is probably due in part to the much smaller number of naturally occurring titanosilicates and to the difficulty associated in synthesizing many of these compounds.

This study was undertaken to determine if systematic chemical shifts in ^{29}Si NMR spectra can be reliably correlated to the number of titanium polyhedra coordinating any given silicon tetrahedron and to the oxygen formal charge. In the first part of the paper, experimentally determined local bonding configurations are compared with bonding configurations predicted from known crystal structures and from a simple formal charge model.[11] From these relationships, shift−structure correlations are established. In the second part of the paper, the chemical shift information from compounds with known crystal structures is used to determine the local bonding configurations for a new titanosilicate zeolite $CsTiSi_2O_{6.5}$ and for an Engelhard zeolite formulation designated ETS-4.

2. Experimental Procedure

2.1. Synthesis. The titanosilicates used in this study were synthesized by a variety of techniques. $Na_2TiSi_4O_{11}$, $CsTiSi_2O_{6.5}$, $Na_2TiSi_2O_7$, and Na_2TiSiO_5 were synthesized from sol gels. For sol gel synthesis, mixtures of tetraethyl orthosilicate (TEOS) and titanium isopropoxide (TIP) were hydrolyzed using a mixture of alkali hydroxide, water, and ethanol. After gelation, additional water was added to break up the gel, and the liquid was stirred and aged overnight. The mixture was slowly dried and then calcined and heat treated under a temperature−time regimen that was optimum for the compound of interest. $Na_2TiSi_4O_{11}$ formed after melting at 1035 °C, grinding, and then heat treating to 800 °C for 12 h. Similarly, $Na_2TiSi_2O_7$ crystallized after melting at 985 °C, grinding, and heat treating to 820 °C for 14 h. $CsTiSi_2O_{6.5}$ and Na_2TiSiO_5 formed directly after heat treatment to 800 °C for 1 h and 900 °C for 12 h, respectively.

$K_2TiSi_3O_9$, $Na_2Ti_2Si_2O_9$, $Cs_2TiSi_6O_{15}$, and $Ba_2TiSi_2O_8$ (fresnoite), were synthesized from mixtures of TiO_2 and SiO_2 and K_2CO_3, Na_2CO_3, Cs_2CO_3, or $Ba(CO_3)$. The powders were mixed using a mortar and pestle and then heat treated. Several cycles of grinding and heat treatment were necessary to form phase-pure compounds. Crystalline $K_2TiSi_3O_9$ and $Na_2Ti_2Si_2O_9$ formed after heat treating powders to 1000 °C for 12 h and 900 °C for 24 h, respectively. Fresnoite crystallized after melting at 1200 °C, cooling to room temperature, and then heat treating at 900 °C for 24 h. The addition of $CsVO_3$ flux was necessary to synthesize $Cs_2TiSi_6O_{15}$. In this case, the component oxides where mixed and melted, ground with flux, and then heat treated at 790 °C for at least 50 h. The mineral forms of $CaTiSiO_5$ (sphene or titanite, Wards Geology, Rochester, NY), $BaTiSi_3O_9$ (benitoite, supplied by the National Museum of Natural History, Smithsonian Institution, benitoite-California-

[⊗] Abstract published in *Advance ACS Abstracts,* October 15, 1997.

S1089-5647(97)01429-6 CCC: $14.00

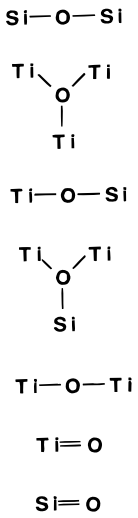

Figure 1. Schematic of typical oxygen bonding configurations in silicates, titanates, and titanosilicates.

87424), and $Na_2TiSi_4O_{11}$ (narsarsukite, supplied by the National Museum of Natural History, Smithsonian Institution, narsarsukite-Greenland-138948) were used, and ETS-4 were obtained from Engelhard Corporation.

2.2. ^{29}Si NMR. The 59.27 MHz ^{29}Si solid-state NMR experiments were carried out with a Chemagnetics spectrometer (300 MHz, 89 mm, wide-bore Oxford magnet) with a double resonance probe. Solid samples were loaded into 7 mm Zirconia PENCIL rotors and spun at 3−4 kHz. Spectra were collected by using a single-pulse Bloch-decay method (with ^{1}H decoupling) with a 5 μs (90°) ^{29}Si pulse and a 60 s repetition delay. For all experiments, 40 ms acquisition times and a 25 kHz spectral window were employed. The number of transients ranged from 2000 to 5000. A Lorentzian line broadening of 50 Hz was used for all spectra. The chemical shifts were referenced to tetramethylsilane at 0 ppm.

3. Results and Discussion

The number of titanium polyhedra that coordinate any given silicon tetrahedron is determined by the Ti−O coordination number, the long-range crystal structure, and the distribution of titanium on any given site within the structure. In general, titanosilicates consist of a covalently bonded "network" of silicon, oxygen, and titanium, and weakly bonded alkali and alkaline earth "modifying" cations that compensate for the net negative charge on the network. Although silicon almost always occurs in a tetrahedral environment at low pressure, titanium can be coordinated by four, five, or six oxygens, and the oxygens can be bonded to one to four network-forming cations. Examples of oxygen coordination environments for bonding to one, two, or three cations are shown in Figure 1. These oxygen coordination environments are designated Si−O−Si, Ti−Ti−Ti, Si−O−Ti, Si−Ti−Ti, Ti−O−Ti, Ti(NBO), and Si(NBO). Assuming all the silicons are bonded to four bridging oxygens (with two bonds to each oxygen), then five distinct silicon environments exist and are designated Si(0Ti), Si(1Ti), Si(2Ti), Si(3Ti), and Si(4Ti). The number of unique environments increases when nonbridging oxygens are included. For example, in the case of silicon with one titanium as the next-nearest neighbor, four possible environments can exist: Si(1Ti), Si(1NBO)(1Ti), Si(2NBO)(1Ti), and Si(3NBO)(1Ti).

The type and number of each bonding configuration can be deduced from the crystal structure, and in turn the environment surrounding the silicon atoms can be determined.[11] In the absence of reliable crystal structure data, the most stable bonding configurations can be predicted by using a simple formal charge model and phase diagram information.[11,15] The formal charge model is based on the assumption that stable structures are dictated by local bonding configurations that satisfy the bonding requirements of all oxygens in the structure. Oxygens are assumed to come closest to having their bonding requirements satisfied if the sum of the positive charges donated to each oxygen by bonding to next-nearest neighbor cations is +2, which is the condition that exactly neutralizes the formal charge on oxygen of −2. In the model, only "network-forming" cations such as Si^{4+} and Ti^{4+}, which have valences greater than or equal to +3, are considered. The "modifying" cations (with a valence of +1 or +2) neutralize any excess negative charge on oxygen sites. The charge donated by the various network-forming cations is taken as the cation charge divided by the cation coordination number as in Pauling's second rule[16] and Brown and Shannon's treatment of bond strengths.[17] For example, in this simple model, octahedrally coordinated Ti^{4+} donates a net charge of $+^4/_6 = +0.67$ to each oxygen to which it is bonded. Tetrahedrally coordinated Si^{4+} donates a charge of +1 to each oxygen. Although the model is described in more detail elsewhere,[11,15] the general rules used to evaluate the relative stability of different oxygen bonding configurations are the following.

(1) Oxygens that carry a net positive charge of greater than +0.5 are relatively unstable. For example, oxygens bonded to four or three tetrahedral Si^{4+} ions (with net oxygen charges of +2 and +1, respectively) should be much less stable than charge neutral Si−O−Si bonds or neutral oxygens bonded to three octahedral Ti^{4+} ions.

(2) Oxygens can carry a net negative charge only if they are charge compensated by ionic bonds to monovalent or divalent modifier cations such as alkali metal or alkaline earth ions. For example, pure silica contains very few oxygens bonded to only one Si^{4+} with a net charge of −1 (NBO). However, sodium silicate materials contain one NBO for each Na^+ in the composition.

(3) The oxide will contain a mixture of structural units that minimize the anionic character on the greatest number of oxygens. For example, in sodium aluminosilicates the model predicts that substitution of Al into tetrahedral sites to make four Si−O−Al bonds (each oxygen having a charge of −0.25) is preferred over the formation of one silicon nonbridging oxygen (with the same net charge of −1).

(4) The number of bonds formed to all species must be consistent with the formula unit and with both cation and anion coordination geometries. For example, for the formula $Na_2Ti_4O_9$, if the titanium has an octahedral coordination geometry, the mix of possible oxygens in the structure must account for a total of (six bonds/Ti) × (4 Ti) = 24 titanium−oxygen bonds. All nine oxygens in the formula unit cannot be neutral oxygens coordinated to three titanium cations as in TiO_2, since this would result in a net of 27 titanium−oxygen bonds.

Titanosilicates can contain anionic sites with a formal charge ranging from −0.2 (for Si−O−Ti(5)) to −1.33 (for Ti(6) NBO). The formal charge model predicts that oxygen sites with the least anionic character should be the most stable. For example considering Ti(6), the relative ease of formation of anionic sites should follow the trend Si−O−Ti > Ti−O−Ti > Si NBO > Ti NBO. However, if the modifier content is high enough, the structure may be incapable of creating a sufficient population of sites having low anionic charge to neutralize all modifier cations. At a fixed Si:Ti ratio, anionic site distributions are expected to move from sites having low charge to those having high charge as the modifier content (and thus the net charge requiring neutralization) increases.

TABLE 1: Experimental ^{29}Si NMR Chemical Shift and Phase Selection for Silicotitanate Mineral and Synthetic Compounds

compound	mineral	origin	phase	chemical shift (ppm) (P_x)	chemical shift (ppm) (P_x)	chemical shift (ppm) (P_x)	chemical shift (ppm) (P_x)
Na_2TiSiO_5	natisite	synthetic	100% Na_2TiSiO_5	−82.1 (36)	−89.1 (21)	−93.6 (21)	−61.7 (22)
$CaTiSiO_5$	sphene	mineral	100% $CaTiSiO_5$	−79.39 (100)			
$Na_2Ti_2Si_2O_9$	lorenzenite or ramsayite	synthetic	96% $Na_2Ti_2Si_2O_9$ + 4% $Na_2Ti_6O_{13}$	−90.8 (100)			
$Na_2TiSi_2O_7$		synthetic	94% $Na_2TiSi_2O_7$ + 6% SiO_2	−90.7 (47)	−87.2 (29)	−82.2 (17)	−61.4 (7)
$Ba_2TiSi_2O_8$			85% $Ba_2TiSi_2O_8$ + 10% $BaTiO_3$ + <5% $BaSiO_3$ + <1% other	−82.1 (93)	−88 (7)		
$BaTiSi_3O_9$	benitoite	mineral	100% $BaTiSi_3O_9$	−94.3 (100)			
$K_2TiSi_3O_9$		synthetic	100% $K_2TiSi_3O_9$	−94.4 (100)			
$Na_2TiSi_4O_{11}$	narsarsukite	synthetic	100% $Na_2TiSi_4O_{11}$	−94.8 (46)	−97.7 (45)		−61.8 (9)
$Na_2TiSi_4O_{11}$	narsarsukite	mineral	100% $Na_2TiSi_4O_{11}$	−97.3 (36)	−99.8 (34)	−104.9 (30)	
Cs_2TiSi_6O15		synthetic	90% $Cs_2TiSi_6O_{15}$ + 10% SiO_2	−99.3 (32)	−101.6 (24)	−102.9 (26)	−110.4 (18)
$CsTiSi_2O_{6.5}$		synthetic	97% $CsTiSi_2O_{6.5}$ + 3% unidentified	−102.1 (49)	−94 (22)	−87.9 (20)	−61.5 (9)
ETS-4		synthetic	similar to zorite	−90.57 (73)	−96.7 (27)		
SiO_2			amorphous	−111.3 (68)	−102.7 (32)		

3.1. ^{29}Si MAS NMR and XRD. X-ray diffraction was used to analyze all mineral and synthetic samples for phase content and purity. A summary of the diffraction results and the isotropic ^{29}Si chemical shifts of natural and synthetic titanosilicates examined in this study is shown in Table 1. The ^{29}Si MAS NMR spectra are shown in Figure 2. The relative amount of each type of silicon environment is shown in Table 1 and was estimated using peak height measurements, $P(x)$,

$$P(x) = 100[I_x/(I_0 + I_1 + I_2 + ...)] \quad (x = 0, 1, 2, 3, \text{or } 4) \quad (1)$$

where I_0, I_1, and I_2 are the peak heights of the MAS NMR line shape components assigned to the respective silicon sites. Below, the experimental chemical shifts shown in Table 1 are reconciled with known titanosilicate crystal structures.

3.2. Reference Compounds. *SiO_2.* The ^{29}Si NMR spectrum for silica is shown in Figure 2b (PPG Industries, Hi-Sil 233, 20 nm amorphous silica particles). Fully condensed SiO_2 polymorphs typically resonate above −100 ppm.[12,13] Nonbridging oxygens cause distinct low-field chemical shifts of about 10 ppm for each added NBO.[12,13] The observed main peak at −111.3 ppm represents silicon with four bridging oxygens, while the shoulder at −102.7 ppm is due to silicon with three bridging oxygens and one NBO. The nonbridging oxygens result from sodium impurity, which acts to break up the covalently bonded Si−O−Si network.

$CaTiSiO_5$ (Sphene or Titanite) and Na_2TiSiO_5 (Natisite). The crystal structure of titanite[18,19] consists of kinked chains of corner-sharing TiO_6 octahedra cross-linked by silicon tetrahedra. The silicon tetrahedra share oxygen atoms with four separate Ti octahedra in three separate chains, and the oxygen atoms are shared by two network-forming cations. All four bonds to silicon are of the type Si−O−Ti, or Si(4Ti). As shown in Figure 2b, the Si(4Ti) bonding configuration for $CaTiSiO_5$ is represented in the experimental ^{29}Si NMR spectrum by a single peak with a chemical shift of −79.39 ppm with spinning sidebands at −27.14 and −131.64 ppm.

The chemical composition of Na_2TiSiO_5 (natisite) is formally related to sphene with two sodiums replacing calcium. However, the titanium environment and crystal structure are very different. Titanium in natisite is coordinated by five oxygens in a square pyramidal geometry. The corners of the square pyramids are shared with four SiO_4 tetrahedra, and at the apex is a nonbridging oxygen.[20,21] The silicon tetrahedra and titanium square pyramids form layers that are separated by Na^+ ions, resulting in a bonding configuration that contains four Si−O−Ti and one Ti−NBO. Because all four bonds to silicon are of the type Si−O−Ti, ^{29}Si NMR is expected to show a single peak representing Si(4Ti). The signal-to-noise ratio for the Na_2TiSiO_5 ^{29}Si NMR experimental spectrum (Figure 2b) is low, with weak, ill-defined peaks. The prominent peak has a chemical shift of −82.1 ppm, and three very weak peaks close to the noise level are detected at −89.1, −93.6, and −61.7 ppm. The peak at −82.1 ppm represents the prevalent silicon environment Si(4Ti). The silicon environment and bond angles are the same for all silicons in the structure, and the XRD showed no crystalline impurity peaks; therefore, it is likely that the lower intensity peaks are due to a minor amount of unreacted, amorphous silicate impurity. The impurity peak at −61.7 ppm is typical of all samples that were fabricated using a sol−gel method. Peaks near this shift range have been shown to represent neosilicate (Si(4NBO) or Q^0) silica monomers in the magnesium, lithium, calcium, sodium, and barium silicates.[22] Therefore, it is likely that one of the minor impurities in synthetic Na_2TiSiO_5 is a sodium silicate or a protonated sodium silicate.

$Na_2Ti_2Si_2O_9$ (Ramsayite or Lorenzenite) and $Na_2TiSi_2O_7$. In lorenzenite, the titanium coordination geometry is octahedral and the silicon tetrahedra form pyroxene-type (Si_2O_6) chains, where two of the oxygen atoms in each tetrahedron are bonded to a silicon. One of the two remaining oxygen atoms in the silicon tetrahedron is bonded to two titanium atoms, while the other is bonded to one titanium atom.[23,24] The total bonding configuration contains two Si−O−Si, two Si−Ti−Ti, two Si−O−Ti, and three Ti−O−Ti, where all the silicon atoms have five next-nearest neighbors, 2Si and 3Ti, or Si(3Ti). The experimental NMR spectrum for this compound exhibits one sharp peak at a chemical shift of −90.8 ppm (Figure 2a), which is representative of Si(3Ti). The XRD results show a minor amount of unreacted crystalline sodium titanate, $Na_2Ti_6O_{13}$, impurity. On the basis of the starting chemical composition, there is likely to be a small amount of amorphous unreacted sodium silicate present, which was undetected by XRD. The very low-intensity shoulder on the main peak may be due to this sodium silicate impurity.

The ternary compound $Na_2TiSi_2O_7$ was discovered in 1979 by Glasser and Marr;[25] however, no crystal structure determination has been performed on this material. In the absence of structural data, the most likely titanium coordination and bonding configurations can be predicted using the formal charge model.[11] The composition lies in a region of the phase diagram where the titanium is predicted to be in octahedral coordina-

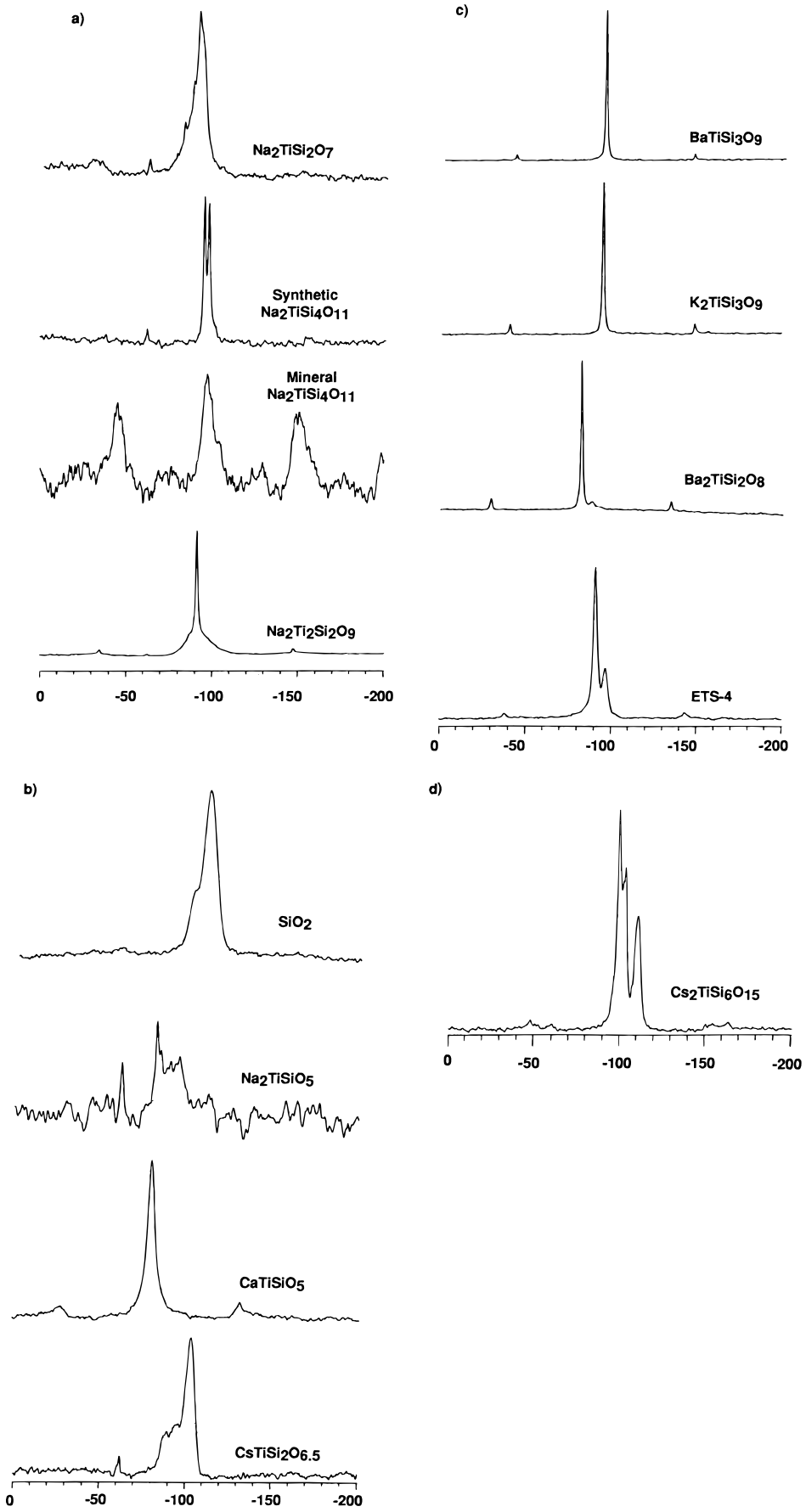

Figure 2. Experimental ^{29}Si NMR spectra for mineral and synthetic titanosilicates. All chemical shifts are referenced to tetramethylsilane at 0 ppm.

tion.[11] Assuming octahedral titanium coordination, there are eight bonds to two silicons and six bonds to one titanium. The possible bonding configurations and their stability ranking (based on the formal charge model)[11] are shown in Table 2. The most stable configuration consists of six Si−O−Ti type bonds and one Si−O−Si, which represents an average Si(3Ti)

TABLE 2: Possible Bonding Configurations for $Na_2TiSi_2O_7$ with Ti(6)[a]

Si−Ti−Ti +1/3	Ti−Ti−Ti 0	Si−O−Si 0	Si−O−Ti −1/3	Ti−O−Ti −2/3	Si-NBO −1	Ti-NBO $-1^1/_3$	*N*	rank
0	0	1	6	0	0	0	7	1
0	0	2	4	1	0	0	6	2
1	0	1	4	0	1	0	5	5
0	1	2	3	0	0	1	6	3
1	0	2	3	0	0	1	5	7
0	0	3	2	2	0	0	5	4
2	0	1	2	0	2	0	3	10
1	1	2	1	0	2	1	4	9
0	1	4	0	1	0	1	5	6
0	2	3	0	0	2	0	5	8
3	0	1	0	0	3	0	1	11

[a] *N* is the number of near-neutral oxygens in the formula unit. The bonding configurations are ranked with "1" being the most stable

bonding configuration (six to eight bonds to Si are Si−O−Ti). The ^{29}Si NMR experimental results show a high-intensity signal at −90.7 ppm, a shoulder at −93.6 ppm (79% relative intensity), and three lower intensity signals at −87.2 ppm (60% relative intensity), −82.2 ppm (42% relative intensity), and −61.4 ppm (16% relative intensity; see Table 1). The chemical shift of the main peak is similar to that of $Na_2Ti_2Si_2O_9$ (−90.8 ppm) and is assigned to a silicon environment with three titanium next-nearest neighbors, Si(3Ti). The shoulder at −93.6 ppm is similar to the shift seen for compounds $BaTiSi_3O_9$ and $K_2TiSi_3O_9$ (see section 3.1) and represents Si(2Ti). The peak at −82.2 ppm is in the shift range of Si(4Ti), and the peak at −87.2 ppm can be assigned to either Si(3Ti) or Si(4Ti). These results indicate that there is more than one crystallographic site for the silicon in this compound, but the majority of the silicon is coordinated by three titanium next-nearest neighbors. XRD analysis shows that the synthetic $Na_2TiSi_2O_7$ sample contained approximately 6% SiO_2 crystalline impurity. Si(NBO) groups in the impurity phase may contribute to the peaks at −87.2 and −82.2 ppm. Magi et al.[12] have shown that Si(2NBO), Q^2, and Si(1NBO), Q^1 resonate in the ranges of −74 to −94 ppm and −67 to −83 ppm, respectively. These peaks may also be due to Ti-rich titanosilicate impurities or from nonstoichiometric Ti-rich $Na_2TiSi_2O_7$ that contains some Si(4Ti). As discussed previously, the NMR peak at −61.4 represents a Q^0 amorphous sodium silicate impurity.

$BaTiSi_3O_9$ (Benitoite) and $K_2TiSi_3O_9$. Benitoite contains octahedral titanium, which connect Si_3O_9 rings.[26] The overall bonding configuration consists of three Si−O−Si and six Si−O−Ti. Therefore, of the 12 available Si−O bonds, six of them are occupied by titanium, which can be designated Si(2Ti). As shown in Figure 2c, the experimental ^{29}Si NMR spectrum of mineral benitoite exhibits one sharp, high-intensity resonance at −94.3 ppm representing a Si(2Ti) environment. This chemical shift is in good agreement with the −94.2 ppm shift determined by Magi et al.[12]

The crystal structure of $K_2TiSi_3O_9$ has not been determined; however, based on composition and the formal charge model, $K_2TiSi_3O_9$ is expected to have bonding configurations similar to those of benitoite. This is confirmed by experimental NMR data for $K_2TiSi_3O_9$ that show a single, high-intensity peak at −94.4 ppm, which is representative of Si(2Ti) (Figure 2c).

$Na_2TiSi_4O_{11}$ (Narsarsukite). The $Na_2TiSi_4O_{11}$ structure consists of chains of titanium octahedra joined by opposite vertexes and $[Si_4O_{10}]$ chains made up of four-membered rings of SiO_4 tetrahedra.[27] The SiO_4 and TiO_6 chains are joined at the vertices, which results in an overall local bonding configuration consisting of six Si−O−Si, four Si−O−Ti, and one Ti−O−Ti. Therefore, out of 16 available Si−O bonds, four are bonded to titanium, thus yielding Si(1Ti). ^{29}Si NMR data collected for both the synthetic and mineral forms of $Na_2TiSi_4O_{11}$ are shown in Figure 2a. The spectrum for the natural mineral sample exhibits weak, ill-defined peaks with a very low signal-to-noise ratio and strong spinning sidebands. These characteristics are probably due to traces of a paramagnetic impurity, such as iron, which is common in naturally occurring narsarsukite minerals.[28] The broad peak for the mineral specimen encompasses the chemical shift range (−91 to −106 ppm) over which two sharp peaks can be observed for the synthetic specimen. Synthetic $Na_2TiSi_4O_{11}$ exhibits two sharp, intense peaks at −94.8 and −97.5 ppm and a weak peak at −61.8 ppm. The presence of two strong peaks is inconsistent with the single-silicon-environment (Si(1Ti)) prediction based on the crystal structure presented by Pjatenko.[27] The peak at −94.8 ppm is at a chemical shift similar to that of Si(2Ti) in benitoite and $K_2TiSi_3O_9$, while the peak at −97.5 ppm is in a range between those of Si(2Ti) and Si(0Ti),[12,13] which is consistent with a Si(1Ti) environment. A 50/50 mixture of Si(2Ti) and Si(1Ti) as shown by the experimental data agrees with the preferential bonding configuration predicted by the formal charge model.[11] Table 3 shows the possible bonding configurations for $Na_2TiSi_4O_{11}$ containing octahedral titanium and also ranks the configurations on the basis of stability. The model predicts a bonding configuration containing five Si−O−Si and six Si−O−Ti, with six out of 16 available Si−O bonds bonded to titanium. The structure by Pjatenko yields the second most stable bonding configuration containing six Si−O−Si, four Si−O−Ti, and one Ti−O−Ti. XRD data of the mineral and synthetic forms of $Na_2TiSi_4O_{11}$, shown in Figure 3 and summarized in Table 1, are identical, showing 100% crystalline narsarsukite with no detectable impurities that could account for the appreciable amount of Si(2Ti). A small amount of sodium silicate monomer, similar to that seen in all other sol−gel prepared samples, is evident in the NMR spectra of the synthetic sample; however, this relatively small impurity cannot explain the apparently large quantity of Si(2Ti). The inconsistency of the experimental ^{29}Si NMR data with the proposed structure, in addition to the agreement of the NMR data with optimum theoretical bonding configurations, warrants a new investigation of the crystal structure of narsarsukite. Pjatenko's original refinement of the crystal structure with a space group of $I4/m$ has a high *R* factor of 13%. A slight distortion of the silicon atoms would result in a noncentrosymmetric cell that can be justified with space group of $I4$ or $I\bar{4}$, and with the presence of two distinct silicon sites with unique bond angles. For the purposes of this investigation, we assume that the resonance at −97.7 ppm represents Si(1Ti), which is consistent with other Si(1Ti) compounds. The resonance at −94.8 ppm, which could be due to either a second Si(1Ti) or Si(2Ti) site, is not assigned a configuration and is not used for the determination of unknown compounds.

$Cs_2TiSi_6O_{15}$. The crystal structure of this titanosilicate consists of an open framework structure of corner-shared silicon tetrahedra and isolated titanium octahedra.[29] The cesium ions are located in large cavities formed by the network. There are 24 bonds to six silicons and six bonds to one titanium with an

TABLE 3: Possible Bonding Configurations for $Na_2TiSi_4O_{11}$ with Ti(6)[a]

Si−Ti−Ti +1/3	Ti−Ti−Ti 0	Si−O−Si 0	Si−O−Ti −1/3	Ti−O−Ti −2/3	Si-NBO −1	Ti-NBO $-1^1/_3$	*N*	rank
0	0	5	6	0	0	0	11	1
0	0	6	4	1	0	0	10	2
1	0	5	4	0	1	0	9	6
0	0	7	2	2	0	0	9	5
0	1	7	2	0	0	1	10	4
0	1	6	3	0	1	0	10	3
0	2	7	0	0	2	0	9	8
0	1	7	1	1	1	0	9	7
1	1	6	1	0	2	0	8	10
2	0	6	1	0	1	1	7	12
3	0	5	0	0	3	0	5	14
2	0	6	0	1	2	0	6	13
1	0	7	0	2	1	0	7	11
0	0	8	0	3	0	0	8	9

[a] *N* Is the number of near neutral oxygens in the formula unit. The bonding configurations are ranked with "1" being the most stable.

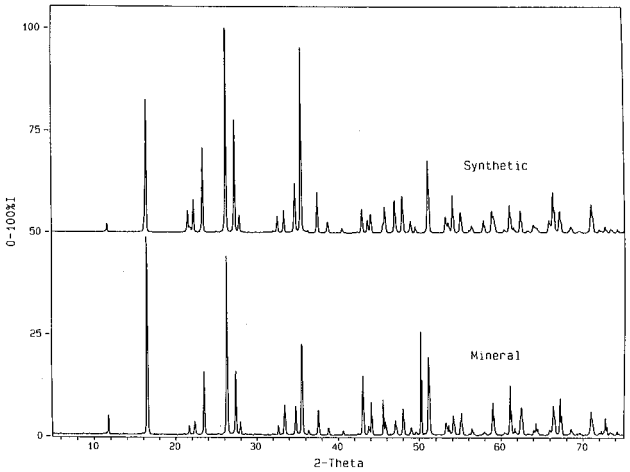

Figure 3. Comparison of the powder X-ray diffraction spectra for mineral and synthetic $Na_2TiSi_4O_{11}$.

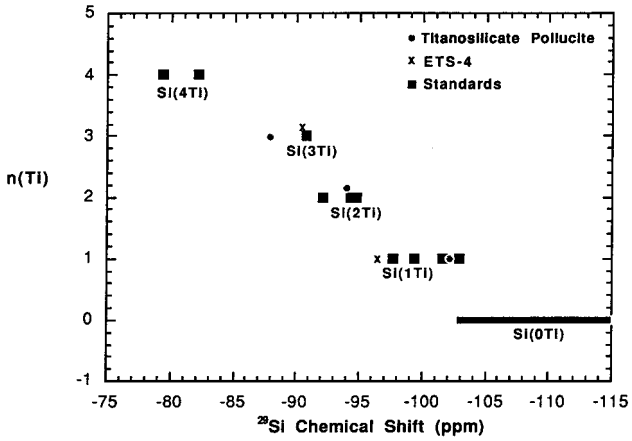

Figure 4. Experimental ^{29}Si NMR chemical shift as a function of the number of titanium neighbors surrounding each Si tetrahedron for titanosilicate standards, $CsTiSi_2O_{6.5}$, and ETS-4 (Engelhard formulation).

overall configuration of nine Si−O−Si and six Si−O−Ti type bonds or Si(1Ti). Crystal structure results show that three silicon sites exist with unique bond angles between neighboring tetrahedra and octahedra.[29] Each of the Si(1Ti) sites has a unique resonance in the ^{29}Si NMR spectra at −99, −102, and −103 ppm (Figure 2d). The ^{29}Si NMR peak at −111 ppm is due to a silica impurity that was present in all powder samples of this compound.

$Ba_2TiSi_2O_8$ (Fresnoite). The crystal structure of fresnoite[30,31] consists of pyrosilicate $[Si_2O_7]^{6-}$ tetrahedral pairs linked to five-coordinate titanium square pyramids. Each silicon tetrahedron is bonded to one other silicon tetrahedron, two titanium square pyramids, and one nonbridging oxygen, resulting in an average bonding configuration containing one Si−O−Si, four Si−O−Ti, two Si(NBO), and one Ti(NBO). Therefore, of the eight bonds to two silicons, four are bonded to titanium-yielding Si(2Ti). Both the nonbridging oxygen and the neighboring titanium polyhedra contribute to the ^{29}Si chemical shift.[12] Magi et al.[12] showed that each addition of nonbridging oxygens to fully condensed SiO_2 results in a ^{29}Si downfield chemical shift of approximately 10 ppm. The experimental spectrum of $Ba_2TiSi_2O_8$ shown in Figure 2c exhibits a strong resonance at −82.1 ppm and a very weak impurity resonance at −88 ppm. Typical experimental chemical shifts for Si(2Ti) are near −94.4 ppm (based on $BaTiSi_3O_9$ (benitoite) and $K_2TiSi_3O_9$). If an approximate downfield shift of −10 ppm from the NBO as well as from the titanium contribution is accounted for, the estimated chemical shift is −84 ppm, which is in good agreement with the observed shift of −82.1 ppm. The weak resonance at −88 ppm is due to minor impurities (<5 wt %) of barium silicates that were detected by XRD (Table 1).

TABLE 4: Local Silicon Bonding Configurations Determined by ^{29}Si NMR and the Summation of the Formal Charge Per Silicon for All Study Compounds

compound	Si(*n*Ti)	formal oxygen charge/Si
Na_2TiSiO_5	Si(4Ti)	−0.8
$CaTiSiO_5$	Si(4Ti)	−1.33
$Na_2Ti_2Si_2O_9$	Si(3Ti)	0
$Na_2Ti_2Si_2O_7$	Si(3Ti)	−1
$Ba_2TiSi_2O_8$	Si(2Ti)	−1.4
$BaTiSi_3O_9$	Si(2Ti)	−0.67
$K_2TiSi_3O_9$	Si(2Ti)	−0.67
$Na_2TiSi_4O_{11}$	Si(1Ti) + Si(1Ti or 2Ti)	−0.33 Si(1Ti)
$Cs_2TiSi_6O_{15}$	Si(1Ti)	−0.33
$CsTiSi_2O_{6.5}$	Si(1Ti) + Si(2Ti) + Si(3Ti)	−0.2 Si(1Ti), −0.4 Si(2Ti), −0.6 Si(3Ti)
ETS-4 (Si/Ti = 2.7)	Si(1Ti) + Si(3Ti)	−0.33 Si(1Ti), −1.0 (Si(3Ti))

The ^{29}Si NMR chemical shift as a function of the number of next-nearest titanium neighbors for all the standard compounds are plotted in Figure 4, and the coordination environments are summarized in Table 4. A systematic downfield shift can be seen with increasing titanium next-nearest neighbors,which is similar to the trend observed in aluminosilicates.[14] The chemical shift ranges for Si(4Ti), Si(3Ti), Si(2Ti), and Si(1Ti) in the figure are based on experimental data obtained in this study, whereas the range defined for Si(0Ti) is based on chemical shifts cited in the literature.[12−14] For the fresnoite sample, the downfield chemical shift contribution from nonbridging oxygens can be estimated at 10 ppm.[12] For the purpose of comparison, in Figure

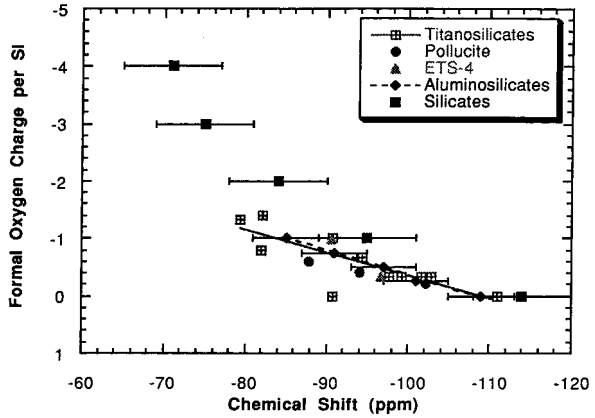

Figure 5. Chemical shift as a function of the sum of the oxygen formal charge per silicon. Chemical shift values for aluminosilicates and silicates are from Lippmaa et al.[13] and Magi et al.,[12] respectively.

4 the chemical shift of fresnoite has been shifted upfield by 10 ppm in order to subtract the contribution from nonbridging oxygens.

The ^{29}Si NMR chemical shift is illustrated in Figure 5 and Table 4 as a function of the sum of the oxygen formal charge per silicon for titanosilicates, aluminosilicates (data collected by Lippmaa et al.[13]), and silicates with different degrees of condensation (data collected by Magi et al.[12]). The sums of the formal charge on the oxygen surrounding each silicon, which is shown in Table 4, were calculated based on the known crystal structures for the compounds. For example, the bonding configuration for $BaTiSi_3O_9$ consists of three Si−O−Si and six Si−O−Ti, or alternatively, each tetrahedral silicon has two titanium next-nearest neighbors and two silicon next-nearest neighbors. Since titanium in octahedral coordination donates a charge of +0.67 ($^4/_6$) to each oxygen, the sum of the formal oxygen charge per silicon is 2 (−0.33) or −0.67. Likewise, the silicon environment in $BaTiSi_2O_8$, with Ti(5), has two Si−O−Ti (formal charge of −0.2), one Si−O−Si type bond, and one NBO (formal charge of −1.0), resulting in a formal charge per silicon of −1.4. For compounds with more than one type of silicon environment, the sum of the formal charge for each unique environment is considered, and the corresponding chemical shift for both silicon types is plotted in Figure 5. The data points for aluminosilicates and silicates represent the average chemical shift within the range of possible shifts. Error bars indicate the approximate shift ranges observed for aluminosilicates and silicates with the same oxygen formal charge. Summation of the formal charge on the oxygen takes into account the effects on the chemical shift from next-nearest neighbor cations with various valance and coordination geometries as well as from nonbridging oxygens. A linear fit with similar slope can be made to both the aluminosilicate and titanosilicate data, as shown in Figure 5. Silicates with high formal charge (greater than two nonbridging oxygens) deviate slightly from the trend observed for aluminosilicates and titanosilicates. One titanosilicate compound, $Na_2Ti_2Si_2O_9$, lies outside the expected chemical shift range based on the calculated formal charge. The reason for this deviation is not clear. The crystal structure of this compound is unique in that it is the only titanosilicate compound studied that has a three-coordinate oxygen (Si−Ti−Ti, formal charge = 0.33).

Systematic downward chemical shifts as a function of cation loading in titanosilicate ion exchange materials have been observed by Poojary et al.[32] In this case, sodium in a compound with the ideal formula, $Na_2Ti_2O_3SiO_4 \cdot H_2O$ was systematically exchanged for a proton, resulting in the compound $H_2Ti_2O_3SiO_4 \cdot H_2O$. At the maximum Na uptake ($Na_{1.64}H_{0.36}Ti_2O_3SiO_4 \cdot H_2O$), the silicon resonates at −80.0 ppm, which is in the shift range of Si(4Ti) compounds. A Si(4Ti) environment is consistent with the silicon environment predicted by the crystal structure. As cations are removed and replaced with protons, a systematic upfield shift is observed with the ^{29}Si chemical shift of the fully protonated form at −98.8 ppm. Similar trends are seen when potassium, cesium, and lithium forms were exchanged with protons. Fully loaded lithium samples exhibited a ^{29}Si chemical shift of −83 ppm, which is similar to that of the sodium (full cesium and potassium loading was not achieved). The downfield shift observed with increased alkali loadings can be attributed to deshielding of silicon atoms by alkali that are positioned between the silicon.[32] In terms of the formal charge model, it appears that protons act to neutralize the oxygen formal charge and push the chemical shift toward those similar to fully condensed Si(OTi) (or Q^4_4). Unlike the ion exchange compounds studied by Poojary et al.,[32] the titanosilicates studied in this investigation have fully occupied, nonexchangeable alkali sites. Therefore, there should be no contribution to the ^{29}Si shifts from partial exchange of alkali ions.

TABLE 5: Atomic Positions and Occupancies for $CsTiSi_2O_{6.5}$

atom type	*x*	*y*	*z*	site	occupancy
Si	0.6621	0.5879	0.125	48g	2/3
Ti	0.6621	0.5879	0.125	48g	1/3
O(1)	0.1042	0.1349	0.7175	96h	1
O(2)	0.706	0.062	0.021	96h	0.06
O(3)	0.791	0.205	0.235	96h	0.023
Cs	0.1250	0.1250	0.1250	16b	1

3.3. Titanosilicate Pollucite. ^{29}Si NMR in conjunction with a number of other techniques was used to characterize a new titanosilicate compound $CsTiSi_2O_{6.5}$. In the following sections results from other techniques are summarized and the NMR chemical shift data from standard compounds are used to elucidate silicon environments in $CsTiSi_2O_{6.5}$ and an Engelhard formulation, ETS-4.

3.3.1. Single-Crystal X-ray and Neutron Diffraction. Powder XRD, single-crystal XRD, and neutron diffraction data show that $CsTiSi_2O_{6.5}$ has a crystal structure isomorphous to the mineral pollucite, $CsAlSi_2O_6$, with titanium, rather than aluminum, substituting on one-third of the silicon sites.[33,34] Atom positions and occupancies as determined by neutron and X-ray diffraction are given in Table 5.[34] In $CsAlSi_2O_6$ and $CsTiSi_2O_{6.5}$, an aluminosilicate or titanosilicate network forms by interconnected rings of four and six tetrahedra. Cesium ions are trapped in large cavities formed by the interconnected rings.[35,36] To maintain the pollucite structure and simultaneously substitute titanium for aluminum, a mechanism for charge compensation such as the presence of Ti^{3+} or of oxygen in excess of six per formula unit is required. X-ray photoelectron spectroscopy and electron paramagnetic resonance show that Ti^{3+} is not present. Neutron diffraction indicates that the charge compensation mechanism is the incorporation of eight extra oxygen atoms per unit cell in two, partially occupied, 96-fold positions (O(2) and O(3) in Table 5), resulting in a stoichiometry represented by the formula $CsTiSi_2O_{6.5}$.[34] Although neutron and X-ray diffraction show that the long-range cubic symmetry is preserved, local distortions occur, as is evidenced by large temperature factors in the neutron diffraction Rietveld refinement. Ionic radius considerations and observed silicon and titanium coordinations dictate that the excess oxygen must be part of the titanium coordination sphere; however, because silicon and titanium are randomly distributed about the 48 g site and because X-ray diffraction is less sensitive to oxygen positions than cesium, titanium, or silicon positions,

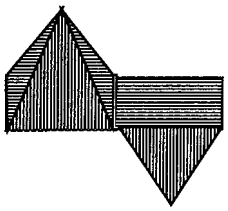

Edge-sharing Ti(5) Pairs

Figure 6. Potential titanium coordination geometries for $CsTiSi_2O_{6.5}$.

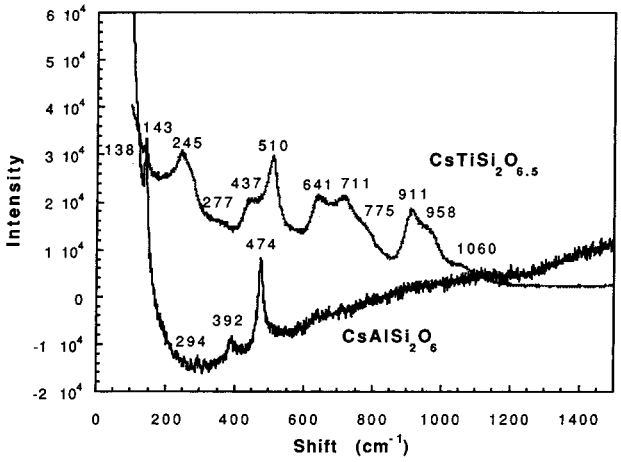

Figure 7. Raman spectra for mineral pollucite, $CsAlSi_2O_6$, and for titanosilicate pollucite, $CsTiSi_2O_{6.5}$.

no conclusions about the distribution of the excess oxygen around the titanium or silicon, or about the individual Si−O and Ti−O bond lengths, could be reached using these techniques.

3.3.2. XAS and Raman of Titanosilicate Pollucite. Other techniques including XAFS, XANES,[37] and Raman spectroscopy were used to probe the local titanium environment in titanosilicate pollucite. Analysis of the EXAFS portion of the titanium spectrum indicates that titanium is coordinated by five oxygens at an average distance of 1.93 ± 0.01. A pre-edge feature in the XANES analysis, which has distinct characteristics for Ti(4), Ti(5), and Ti(6), has been used in the literature to make empirical comparisons and determinations of titanium coordinations in unknowns.[38] A comparison of the intensity and energy shift of this pre-edge feature for $CsTiSi_2O_{6.5}$ with those of standards with known crystal structures shows that $CsTiSi_2O_{6.5}$ lies in a general region where the prevalent titanium coordination is Ti(5); however, the energy shift is closer to compounds containing Ti(4).[37]

The Raman spectra of titanosilicate pollucite (TSP) and mineral pollucite ($CsAlSi_2O_6$) are shown in Figure 7. The spectrum of $CsAlSi_2O_6$ has one prevalent feature at a shift of 474 cm^{-1} that is typical of Si−O type bonds, with minor peaks at 392, 294, and 143 cm^{-1}.[39] The Raman spectrum of TSP exhibits many more peaks than aluminosilicate pollucite, presumably as a result of the distorted local environments around the titanium and silicon atoms. Wilson[40] has shown that the force constants for stretching frequencies are about 10 times greater than those of bending frequencies, which is expressed in terms of vibrational frequencies as

$$\upsilon_{\text{bending}} \approx 0.316\upsilon_{\text{stretching}} \quad (2)$$

From this relationship, it can be shown that the observed peak at 149 cm^{-1} for $CsAlSi_2O_6$ is the bending mode of the peak at 474 cm^{-1}. The peaks observed in the TSP spectrum can be best interpreted by comparing them to those of titanate and silicate reference materials. The peaks at 911, 641, 510, 437, and 268 cm^{-1} observed in the TSP spectrum correlate well with those seen for the Ti(5) compound, $K_2Ti_2O_5$, which exhibits Raman peaks at 899, 650, 534, 461, 323, 287, 224, 192, and 155 cm^{-1}.[41] The prominent peaks at 911 and 510 cm^{-1} are not seen for silicates and are strong evidence for the presence of five-coordinated titanium; however, the peak near 437 cm^{-1} is commonly seen for silicates.[39]

Raman frequencies near 950 and 1100 cm^{-1} have been observed for silica zeolites with small amounts of tetrahedral titanium and for titanium silicate glasses with Ti(4).[42,43] Iwamoto et al.[42] showed that potassium silicate glasses exhibit new peaks at 980 and 770 cm^{-1} upon addition of titanium and interpreted these peaks as Ti(4). Deo et al.[43] showed that the intensity of a band at ∼960 cm^{-1} increases and a minor band at 1125 cm^{-1} forms with addition of Ti(4) to a silica zeolite (TS-1 and TS-2). Based on Iwamota's and Deo's results, the band observed in the TSP spectrum at 958 cm^{-1} could be interpreted as evidence for Ti(4); however, this peak is also known to represent tetrahedral silicon bonding. Further evidence for Ti(4) may be present in the two peaks at 775 and 711 cm^{-1} that are also observed in the Ti(4) compound $BaTiO_4$.[41,44] However, peaks near this shift range have also been observed in alkali and alkaline earth modified silicate glasses. Therefore, although there is evidence for both Ti(4) and Ti(5) in the Raman spectra, the results are inconclusive because of the multiple interpretations for the same set of peaks. Note that the minor peak near 1060 cm^{-1} observed in the TSP spectrum is commonly observed for alkali-modified silica and is representative of a Si−NBO. The Si−NBO signal originates from a minor amorphous cesium−silicate impurity, which was also observed by NMR.

^{29}Si NMR data in conjunction with XAS, Raman, X-ray diffraction, and neutron diffraction data can be used to elucidate the titanium coordination geometry in $CsTiSi_2O_{6.5}$. The ^{29}Si NMR spectrum for $CsTiSi_2O_{6.5}$ is shown in Figure 2b, and the chemical shifts for each peak are overlaid on Figures 4 and 5 and are listed in Table 1. The spectrum exhibits three peaks, with chemical shifts that most closely correspond to standards containing Si(1Ti) (−102.1 ppm), Si(2Ti) (−94 ppm), and Si(3Ti) (−87.9 ppm) environments. A weak peak at −61.5 ppm is assigned to a minor impurity of cesium silicate monomer. Assuming that the intensity of the observed peaks corresponds to the relative quantity of each type of coordination, approximately 54% of the sites are Si(1Ti), 24% are Si(2Ti), and 22% are Si(3Ti). For compounds where the oxygen is bonded to two cations and the silicon is bonded to four bridging oxygens, the number of Si−O−Ti and Si−O−Si type bonds can be determined from the observed distribution of *n* number of titaniums coordinating any given silicons by

$$\text{Si}(n\text{Ti}) \rightarrow n(\text{Si}-\text{O}-\text{Ti}) + [(4-n)/2](\text{Si}-\text{O}-\text{Si}) \quad (3)$$

From eq 3 and from the relative quantities of each coordination type predicted by the experimental spectra, the number of Si−O−Ti (*x*) and Si−O−Si (*y*) bonds in TSP is

$$x\text{Si}-\text{O}-\text{Ti} + y\text{Si}-\text{O}-\text{Si} = 0.54(1\text{Si}-\text{O}-\text{Ti} + {}^3/_2\text{Si}-\text{O}-\text{Si}) + 0.24(2\text{Si}-\text{O}-\text{Ti} + 1\ \text{Si}-\text{O}-\text{Si}) + 0.22(3\text{Si}-\text{O}-\text{Ti} + {}^1/_2\text{Si}-\text{O}-\text{Si})$$

$$= 1.68\text{Si}-\text{O}-\text{Ti} + 1.16\text{Si}-\text{O}-\text{Si}$$

This represents a mixture of 59% Si−O−Ti and 41% Si−O−Si.

TABLE 6: Bonding Configurations for Mixed 50% Tetrahedral (Ti(4)) and 50% Pentacoordinate (Ti(5)) Titanium in $CsTiSi_2O_{6.5}$ (25 Bonds to 13 Oxygens)[a]

50/50 Ti(4) + Ti(5)	Si−O−Si	Si−O−Ti	Ti−O−Ti	Si−NBO	Ti−NBO
		Isolated Ti(5) and Ti(4)			
charge	0	4(0) + 4(−0.2)	−0.2	−1	−1.2
n	4 (33%)	8 (67%)	0	0	1
		Corner-Shared Ti(4) and Ti(5)			
charge	0	3(0) + 3(−0.2)	−0.2	−1	−1.2
n	5 (45%)	6 (55%)	1	0	1
		Edge-Shared Ti(4) and Ti(5)			
charge	0	2(0) + 2(0.2)	0.2	−1	−1.2
n	6 (60%)	4 (40%)	2	0	1

[a] Si−Ti−Ti configurations are not considered.

TABLE 7: Bonding Configurations for All Pentacoordinate Titanium (Ti(5)) in $CsTiSi_2O_{6.5}$ (26 Bonds to 13 Oxygens)[a]

type of bonding charge	Si−Ti−Ti 0.6	Si−O−Si 0	Si−O−Ti −0.2	Ti−O−Ti −0.4	Si−NBO −1	Ti−NBO −1.2
	0	3 23%	10 71%	0	0	0
	0	4 33%	8 67%	1	0	0
	0	5 45%	6 55%	2	0	0
	2	5 55%	4 44%	0	0	2

[a] Si−Ti−Ti type bonding is included but is not likely for Ti(5) compounds.

As shown by neutron diffraction analysis, to maintain charge balance with Ti^{4+} substituted for Al^{3+}, eight additional oxygens must be present in each pollucite unit cell, which contains 16 Ti atoms. There are several possible titanium coordination geometries and bonding configurations that satisfy both charge balance and geometrical constraints. Tables 6 and 7 show the potential bonding configurations for compounds with a 50/50 mix of Ti(4) and Ti(5) or all Ti(5). Configurations that contain triple-bonded oxygen, Si−Ti−Ti, are not included because these oxygens are seriously overbonded (formal charge of +1 for Ti(4) and +0.6 for Ti(5)) and because this configuration is inconsistent with the crystal structure of pollucite and with structures of all known Ti(4)- and Ti(5)-containing compounds. Octahedral titanium (Ti(6)) is not considered for two reasons: (1) XAS results that indicate the presence of Ti(5) (primarily) and Ti(4) (possibly) and (2) crystal structure constraints dictate that the pollucite structure cannot accommodate two additional oxygens near the titanium tetrahedral site.

The observed distributions as determined by NMR and the coordination geometries represented in Tables 6 and 7 can be correlated by comparing the number and type of bonding configurations. On initial inspection two cases, a mixed Ti(4) and Ti(5) and an all Ti(5) coordination geometry with 55% Si−O−Ti and 45% Si−O−Si type bonds, are in good agreement with the observed bonding configuration of 59% Si−O−Ti and 41% Si−O−Si. However, silicon bonds to Ti(4) have a formal charge of zero and are not expected to contribute significantly to the ^{29}Si NMR chemical shift. This conclusion is supported by experimental evidence on silicalites with the MFI structure (TS-1) that shows incorporation of less than 4% tetrahedral titanium into the silicate network causes the Si Q^4 peak at −113 ppm to broaden.[45,46] Addition of 4−14% titanium results in the appearance of a new peak at −116 ppm.[45,46] Therefore, we suspect that fully condensed tetrahedral silicon bonded to tetrahedral Ti^{4+} neighbors in $CsTiSi_2O_{6.5}$ would exhibit a chemical shift in the range −106 to −119 ppm, similar to a fully condensed silicate. If we assume that the Ti(4) Ti−O−Si type bonds do not contribute to the downfield chemical shift, then for the mixed Ti(4) and Ti(5) case, there is the equivalent of 6.5 Si−O−Si and three Si−O−Ti or 68% Si−O−Si and 32% Si−O−Ti. This bonding configuration as well as the other mixed Ti(4) and Ti(5) and all Ti(4) configurations cannot be justified with the experimental data.

TABLE 8: Potential Silicon Bonding Configurations for Edge-Shared Square Pyramidal Ti(5)

no. of Si with Si(*n*Ti) distribution (4Si total) ≈ relative intensity				
Si(0Ti)	Si(1Ti)	Si(2Ti)	Si(3Ti)	Si(4Ti)
0	2	2	0	0
2	0	1	0	1
2	0	0	2	0
1	1	1	1	0
1	0	3	0	0
0	3	0	1	0

The bonding configuration that most closely matches the observed distribution of sites (59% Si−O−Ti and 41% Si−O−Si) contains all Ti(5) with 10 bonds to two titaniums, two of which are of the type Ti−O−Ti and six of which are Ti−O−Si, resulting in an overall bonding configuration containing two Ti−O−Ti, six Ti−O−Si, and five Si−O−Si or 55% Ti−O−Si and 45% Si−O−Si (Table 7). To achieve a pentacoordinate geometry for every titanium, the oxygen must be shared by two edge-sharing titanium square pyramids as shown in Figure 6. If the titanium is evenly distributed about the silicon, this configuration necessitates at least two silicon environments equivalent to a mixture of 50% Si(1Ti) and 50% Si(2Ti). Because the Lowenstien avoidance rule, which is commonly applied to aluminosilicate zeolites, does not apply to titanosilicates, the lowest energy configuration does not necessarily result from an even distribution of titanium around the silicon tetrahedra, and any one of the mixtures of silicon environments shown in Table 8 are possible.

3.4. ETS-4. ETS-4 is a microporous crystalline titanosilicate developed by Engelhard that exhibits a structure similar to zorite, $Na_6[Ti(Ti_{0.9}Nb_{0.1})_4(Si_6O_{17})_2(O,OH)_5]\cdot 11H_2O$.[47,48] The approximate chemical formula of ETS-4 is $M_6Ti_3Si_8O_{25}$, where M is sodium or potassium.[47] The structure proposed by Kuznicki et al.[47] contains Ti(6) exclusively; however, zorite contains a mix of Ti(5) and Ti(6). Assuming the presence of Ti(6) only, there are 32 bonds to eight silicons and 18 bonds to three titaniums, resulting in a preferred bonding configuration containing 18 Si−O−Ti and seven Si−O−Si (72% Si−O−Ti and 28% Si−O−Si) based on the formal charge model. The experimental ^{29}Si NMR spectrum shows two well-defined peaks at −90.57 and −96.68 ppm representing silicon environments of Si(3Ti) and Si(1Ti). From the intensity ratio of the two experimental peaks, ETS-4 contains 73% Si(3Ti) and 27% Si(1Ti). Assuming each oxygen is bonded to two cations and by use of eq 3, the experimental data yield a bonding configuration containing 76% Si−O−Ti and 24% Si−O−Si type bonds, which is in good agreement with the bonding configuration and Ti(6) coordination predicted by the formal charge model and by Kuznicki.[47]

4. Conclusions

Correlations between crystal structure information and experimental ^{29}Si NMR data show that a systematic downfield chemical shift occurs with an increasing number of titanium polyhedra coordinating a given silicon tetrahedron. The ^{29}Si chemical shift increases linearly with increasing oxygen formal charge for both titanosilicates and aluminosilicates. It is convenient to illustrate the chemical shift as a function of oxygen formal charge because summation of the formal charge accounts for affects on the chemical shift from next-nearest neighbor cations with different valance and coordination geometries as well as from nonbridging oxygens. Silicates with a low degree of condensation or high oxygen formal charge deviate from the linear trend observed for aluminosilicates and titanosilicates.

^{29}Si NMR chemical shift data for $CsTiSi_2O_{6.5}$, a new titanosilicate zeolite, support a Ti(5) edge-shared square pyramidal environment, which is in good agreement with the titanium environment predicted from XAS analysis and neutron diffraction measurements. The local bonding configurations predicted by the formal charge model for ETS-4 (unsolved crystal structure) are in agreement with experimental ^{29}Si NMR bonding configurations.

Acknowledgment. The authors gratefully acknowledge David McCready for performing X-ray diffraction measurements, Dr. Nancy Hess for performing and interpreting XAS results, and Dr. Michael Thompson for many fruitful discussions. We also thank Dr. Bob Roth, Dr. Tony Santoro, and Dr. Qing Huang of NIST for performing neutron diffraction experiments and for assistance in determining the structure of pollucite. This work was supported by the Strategic Environmental Research and Development Program (SERDP) and by the Department of Energy's Basic Energy Science (BES), Materials Science program. Pacific Northwest National Laboratory is operated for the U.S. Department of Energy by Battelle under Contract DE-AC06-76RLO 1830.

References and Notes

(1) Clerici, M. G.; Bellussi, G.; Romano, U. Synthesis of Propylene Oxide form Propylene and Hydrogen Peroxide Catalyzed by Titanium Silicate. *J. Catal*. **1991**, *129*, 159−167.

(2) Huybrechts, D. R. C.; De Bruydker, L.; Jacobs, P. A. Oxyfunctionalization of Alkanes with Hydrogen Peroxide on Titanium Silicalite. *Nature* **1990**, *345*, 240−242.

(3) Anthony, R. G.; Phillip, C. V.; Dosch, R. G. Selective Adsorption and Ion Exchange of Metal Cations and Anions with Silico-Titanates and Layered Titanates. *Waste Manag*. **1993**, *13*, 503.

(4) Jentys, A.; Catlow, C. R. A. Structural Properties of Titanium Sites in Ti-ZSM5. *Catal. Lett*. **1993**, *22*, 251−257.

(5) Pei, S.; Zajac, G. W.; Kadnuk, J. A.; Faber, J. Re-investigation of Titanium Silicatalite by X-ray Absorption Spectroscopy: are the Novel Titanium Sites Real? *Catal. Lett*. *21*, 333−334.

(6) Blasco, T.; Camblor, M. A.; Corma, A.; Perez-Pariente, J. The State of Ti in Titanoaluminosilicates Isomorphous with Zeolite β. *J. Am. Chem. Soc*. **1993**, *115* (25), 11806−11813.

(7) Bordiga, S.; Boscherini, F.; Coluccia, S.; Genoni, F.; Lamberti, C.; Leofanti, G.; Marchese, L.; Petrini, G.; Vlaic, G.; Zecchina, A. XAFS Study of Ti-silicalite: Structure of Framework Ti(IV) in Presence and Absence of Reactive Molecules (H_2O, NH_3). *Catal. Lett*. **1994**, *26*, 195−208.

(8) Trong On, D.; Bittar, A.; Sayari, A.; Kaliaguine, S.; Bonneviot, L. Novel Titanium Sites in Silicates. *Catal. Lett*. **1992**, *16*, 85−95.

(9) Sankar, G.; Rey, F.; Thomas, J. M.; Greaves, G. N.; Corma, A.; Dobson, B. R.; Dent, A. J. Probing Active Sites in Solid Catalysts for the Liquid-phase Epoxidation of Alkenes. *J. Chem. Soc., Chem. Commun*. **1994**, 2279−2280.

(10) Behrens, P.; Felsche, J.; Vetter, S.; Schulz-Ekloff, G.; Jaeger, N. I.; Niemann, W. A XANES and EXAFS Investigation of Titanium Silicalite *J. Chem. Soc., Chem. Commun*. **1991**, 678−680.

(11) Bunker, B. C.; Balmer, M. L. Predicting Structures and Properties of Silicotitanate Materials. *Chem. Mater*., submitted.

(12) Magi, M.; Lippmaa, E.; Samoson, A.; Engelhardt, G.; Grimmer, A. R. Solid-State High-Resolution Silicon-29 Chemical Shifts in Silicates *J. Phys. Chem*. **1984**, *88* (8), 1518−1522.

(13) Lippmaa, E.; Magi, M.; Samoson, A.; Engelhardt, G.; Grimmer, A. R. Structural Studies of Silicates by Solid-State High Resolution ^{29}Si NMR. *J. Am. Chem. Soc*. **1980**, *102* (15), 4489−4493.

(14) Lippmaa, E.; Magi, M.; Samoson, A.; Tarmak, M.; Engelhardt, G. Investigation of the Structure of Zeolites by Solid-State High-Resolution ^{29}Si NMR Spectroscopy. *J. Am. Chem. Soc*. **1981**, *103*, (17), 4992−4996.

(15) Bunker, B. C.; Kirkpatrick, R. J.; Brow, R. K. Local Structure of Alkaline-Earth Boroaluminate Crystals and Glasses: I, Crystal Chemical Concepts-Structure Predictions and Comparisons to Known Crystal Structures. *J. Am. Ceram. Soc*. **1991**, *74*(6), 1425−1429.

(16) Pauling, L. *The Nature of the Chemical Bond*, 3rd ed.; Cornell University Press: Ithaca, NY, 1960.

(17) Brown, I. D.; Shannon, R. D. *Acta Crystallogr*. **1973**, *A29*, 266.

(18) Zachariasen, W. H. The Crystal Structure of Titanite. *Z. Kristallogr*. **1930**, *73*, 7−16.

(19) Alexander Speer, J.; Gibbs, G. V. The crystal Structure of Synthetic Titanite, $CaTiOSiO_4$, and the Domain Textures of Natural Titanites. *Am. Mineral*. **1976**, *61*, 238−247.

(20) Nyman, H.; O'Keefe, M. O. Sodium Titanium Silicate, Na_2TiSiO_5. *Acta Crystallogr*. **1978**, **B34**, 905−906.

(21) Nikitin, A. V.; Ilyukhin, V. V.; Litvin, B. N.; Mel'nikov, O. K.; Belov, N. V. Crystal Structure of Synthetic $Na_2(TiO)[SiO_4]$. *Sov. Phys. Dokl*. **1965**, *9* (8), 625−627.

(22) Gunter; Engelhardt, Dieter Michel, *High-Resolution Solid-State NMR of Silicates and Zeolites*; John Wiley and Sons: New York, 1987.

(23) Sundberg, M. R.; Lehtinen, M.; Kivekas, R. Refinement of the Crystal Structure of Ramsayite (Lorenzenite). *Am. Mineral*. **1987**, *72*, 173−177.

(24) Ch'in-hang; Simonov, M. A.; Belov, N. V. The Crystalline Structure of Ramsayite $Na_2Ti_2Si_2O_9 = Na_2Ti_2O_3(Si_2O_6)$. *Sov. Phys. Dokl*. **1969**, *14*, (6), 516−519.

(25) Glasser, F. P.; Marr, J. Phase Relations in the System Na_2O-TiO_2-SiO_2. *J. Am. Cer. Soc*. **1979**, *62*, (1−2), 42−47.

(26) Fischer, K. Verfeinerung der Kristallstruktur von Benitoit $BaTi[Si_3O_9]$. *Z. Kristallogr*. **1969**, *129*, 222−243.

(27) Pjatenko, J. A.; Pudovkna, Z. V. Crystal Structure of Narsarsukite. *Kristallografiya* **1960**, *5*, 563−573.

(28) Wagner, C.; Parodi, G. C.; Semet, M.; Robert, J. L.; Berrahma, M.; Velde, D. Crystal Chemistry of Narsarsukite. *Eur. J. Mineral*. **1991**, *3*, 575−585.

(29) Grey, I. E.; Roth, R. S.; Balmer, M. L. The Crystal Structure of $Cs_2TiSi_6O_{15}$. *J. Solid State Chem*., in press.

(30) Moore, P. B.; Louisnathan, J. Fresnoite, Unusal Titanium Coordination. *Science*, **1967**, *156*, 1361−1362.

(31) Masse, R.; Grenier, J.-C.; Durif, A. Structure Cristalline de la Fresnoite. *Bull. Soc. Fr. Mineral. Cristallogr*. **1967**, *90*, 20−23.

(32) Poojary, D. M.; Bortun, A. I.; Bortun, L. N.; Clearfield, A. Structural Studies on the Ion-Exchanged Phases of a Porous Titanosilicate, $Na_2Ti_2O_3SiO_4{\cdot}2H_2O$. *Inorg. Chem*. **1996**, *35*, 6131−6139.

(33) McCready, D. E.; Balmer, M. L.; Keefer, K. D. Experimental and Calculated X-ray Powder Diffraction Data for Cesium Titanium Silicate, $CsTiSi_2O_{6.5}$: A New Zeolite. *Powder Diffr*. **1997**, *12* (1), 40−46.

(34) Balmer, M. L.; Huang, Q.; Wong-Ng, W.; Roth, R. S.; Santoro, A. Neutron and X-ray Diffraction Study of $CsTiSi_2O_{6.5}$. *J. Solid. State Chem*. **1997**, *130*, 97−102.

(35) Beger, R. M. The Crystal Structure and Chemical Composition of Pollucite. *Z. Kristallogr*. **1969**, *129*, 280−302.

(36) Newnham, R. E. Crystal Structure and Optical Properties of Pollucite. *Mineral. Notes* **1967**, *32*, 1515−1518.

(37) Hess, N. J.; Balmer, M. L. Ti XAS of a Novel Cs-Ti-Silicate. *J. Solid. State Chem*. **1997**, *129*, 206−213.

(38) Waychunas, G. A. Synchrotron Radiation XANES Spectroscopy of Ti in Minerals: Effects of Ti Bonding Distances, Ti Valence, and Site Geometry on Absorption Edge Structure. *Am. Mineral*. **1987**, *72*, 89−101.

(39) McMillan, P. Structural Studies of Silicate Glasses and Melts-Applications and Limitations of Raman Spectroscopy. *Am. Mineral*. **1984**, *69*, 622−644.

(40) Wilson, E. B., Jr.; Decius, J. C.; Cross, P. C. *Molecular Vibrations: The Theory of Infrared and Raman Vibrational Spectra*; Dover: New York, 1980.

(41) Hardcastle, F. D.; Klesnar, H.; Peden, C. F. Structure Refinement of $K_2Ti_2O_5$ by Raman Spectroscopy and X-ray Powder Diffraction. *J. Solid State Chem*., submitted.

(42) Iwamoto, N.; Tsunawaki, Y. Raman Spectra of K_2O-SiO_2 and K_2O-SiO_2-TiO_2 Glasses. *J. Non-Cryst. Solids* **1975**, *18*, 303−306.

(43) Deo, G.; Turek, A. M.; Wachs, I. E.; Huybrechts, D. R. C.; Jacobs, P. A. Characterization of Titania Silicalites. *Zeolites* **1993**, *13*, 365−373.

(44) Wu, K. K.; Brown, I. D. The Crystal Structure of β-Ba_2TiO_4, and the Bond Strength-Bond Length Curve of Ti-O. *Acta Crystallogr*. **1973**, *B29*, 2009.

(45) Thangaraj, A.; Kumar, R.; Mirajkar, S. P.; Ratnasamy, P. Catalytic Properties of Crystalline Titanium Silicalites. *J. Catal*. **1990**, *130*, 1−8.

(46) Reddy, J. S.; Kumar, R.; Ratnasamy, P. Titanium Silicalite-2: Synthesis, Characterization and Catalytic Properties. *Appl. Catal*. **1990**, *58*, L1.

(47) Kuznicki, S. M.; Thrush, K. A.; Allen, F. M.; Levine, S. M.; Hamil, M. M.; Hayhurst, D. T.; Mansour, M. Synthesis and Adsorptive Properties of Titanium Silicate Molecular Sieves. In *Synthesis of Microporous Materials, Vol. 1-Molecular Sieves*; Ocelli, M. L., Ed.; Van Nostrand Reinhold: New York, 1992; p 427.

(48) Sandomirskii, P. A.; Belov, N. V. The OD Structure of Zorite. *Sov. Phys. Crystallogr* **1979**, *24*, 686−693.